Ozawa et al. *EPJ Techniques and Instrumentation* (2024) 11:3
https://doi.org/10.1140/epjti/s40485-024-00111-1

EPJ Techniques and Instrumentation

EPJ.org

RESEARCH ARTICLE

Open Access

Conception, modelling, and characterization of a fiber amplifier with a simple and easy-to-repair configuration intended for the use in harsh environments

Naoya Ozawa[1,3*], Keisuke Nakamura[2] and Yasuhiro Sakemi[2]

*Correspondence:
ozawa.naoya.6t@kyoto-u.ac.jp
[1]Graduate School of Science, University of Tokyo, Hongo 7-3-1, Bunkyo, 113-0033, Tokyo, Japan
[3]*Present address:* Graduate School of Science, Kyoto University, Kita-Shirakawa-Oiwake-cho, Sakyo, 606-8502, Kyoto, Japan
Full list of author information is available at the end of the article

Abstract

We have developed a Yb-doped fiber amplifier (YDFA) using fusion splicing, and characterized its performance with numerical simulation, achieving a continuous output of above 10 W of 1064 nm light. The device has been conceptualized to have a configuration as simple as possible; a strategy for using fiber amplifiers in harsh environments where quick repairs and replacements may become necessary at unexpected times.

Keywords: Fiber amplifier; Fusion splicing; Yb-doped fiber; Radiation; Laser cooling and trapping; Precision measurement

1 Introduction

We have developed a Yb-doped fiber amplifier (YDFA) [1] aimed at use in harsh environments such as accelerator facilities. While the technical breakthroughs in the context of YDFA's have been characterized mainly by output powers, linewidths, and transverse modes [2, 3], our approach aims to achieve a modest performance with a system that is configured as simple as possible, proposing a practical solution for accelerator-based experiments requiring the use of a high-power laser source.

Optoelectric components including semiconductor lasers are suspected to be vulnerable to radiation damage [4]. Although such components are replaceable in principle, it is not efficient in terms of cost and time if the laser source itself has to be sent back to the factory for repair every time, despite the limited beam time. Thus in such cases, commercial laser sources tend to be placed far away from the beamline in a separate room for safety. The light may be sent to the experimental chamber either by free-space transport or through an optical fiber, but in the particular cases where the experimental hall is shared among multiple users and the free-space transport of light becomes a safety issue for them, or the layout of the experimental hall makes the free-space transport unpractical, the use of optical fibers is inevitable [5]. However, long optical fibers cannot support high powers necessary for optical dipole traps due to stimulated Brillouin scattering (SBS) [6], so it is

Springer

unavoidable to place high-power laser sources, including optical amplifiers, close to the beamline. Our solution to this dilemma is to use a self-tailored YDFA instead of a commercially available product. By assembling the amplifier by ourselves, we can prepare the components beforehand and rapidly replace them when needed. Also, the configuration may be customized whenever we find the need for it.

We expect that this approach will be advantageous for experiments aiming to use high-power lasers in accelerator facilities. In often cases, the experimental hall is shared among multiple users, and quantitative estimation of the total radiation damage on the YDFA is not straightforward, thus one cannot completely mitigate the risk of damage. The time slot of the experiments (beam time) is determined a few months prior to the actual experiment, so in an unfortunate occasion where the YDFA is damaged just before the beam time, a rapid repair with minimal additional cost is desired. If the YDFA is made of readily available components and can be disassembled and reassembled by the experimenters themselves, cancellation of the beam time can be avoided, which is a matter of great importance in the field.

One application of this development is the optical trapping of short-lived isotopes. We plan to trap francium (^{210}Fr) atoms in an optical lattice. This system is expected to serve as a probe for fundamental symmetry violation search [7]. As Fr does not have any stable isotope, it is produced using nuclear reactions at the RIKEN Nishina Center (RNC) accelerator facility [8]. In a related study conducted at Tohoku University, the typical neutron flux near the beamline during Fr production is estimated to be on the order of 10^6 cm^{-2}s^{-1}, under the assumption that the neutrons are monochromatic at 1 MeV energy [9]. According to a past study on neutron radiation effects on Yb-doped fibers, the output power is observed to degrade by around 10% after experiencing a total fluence of 10^{14} cm^{-2} of 1 MeV-equivalent monochromatic neutrons [10]. Assuming that the total dose determines the degree of attenuation, our YDFA is expected to decay in output power by 1% in approximately four months. As the Fr experiment plans to accumulate data for several months total in the physics measurement campaign, and there could be additional effects from gamma rays and radiation from other users' experiments, it is crucial that we are always prepared to repair degraded or damaged components with minimal losses of time and cost. In this paper, we describe the setup and procedures of the manufacturing of YDFA, as well as the outcomes of the development.

2 Development

2.1 Requirements for the performance

The YDFA must be capable of producing sufficient laser power for trapping the Fr atoms. At the same time, however, the photon scattering rate must be suppressed so that the trap lifetime does not get shorter than the desired interaction time of ~ 5 s. In order to achieve this, we aim for a trap at the wavelength 1064 nm of 2 W/axis focused to a $1/e^2$ radius of 60 μm. This corresponds to the trap potential depth of approximately 0.2 mK and a photon scattering rate of 0.2 Hz. Roughly estimating that about half of the produced power could be lost by passing through multiple optical components between the YDFA and the vacuum chamber, the required power would be at least ~ 4 W. As the optical fiber used in the amplification stage is a large-mode-area fiber, the transverse mode of the output beam is expected to contain finite contributions from higher-order modes. Since we transport the beam to the vacuum chamber by recoupling it to a single-mode fiber, the

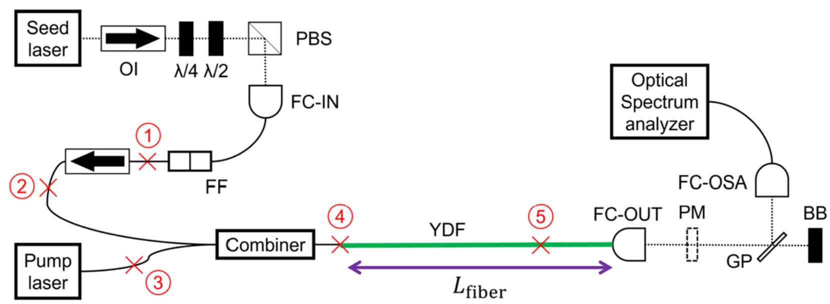

Figure 1 Optical system of the YDFA. Abbreviations are *OI*: optical isolator, *PBS*: polarization beam splitter, *FC*: fiber coupler, *FF*: fiber-to-fiber connector, *PM*: power meter, *GP*: glass plate, and *BB*: beam block. The splice points of the optical fiber are denoted with crosses and label numbers. In particular, splice points 4 and 5 connect the YDF, depicted in the bold green line

beam reaching the chamber is expected to be mode-filtered, regardless of the beam mode at the YDFA output. In practical terms, it is satisfactory if the coupling efficiency of the YDFA output beam to a single-mode fiber is at least 50%, so we use this parameter as a measure for the output beam quality.

2.2 Setup

The configuration of the YDFA is shown in Fig. 1. The seed light of continuous-wave (CW) linearly polarized 1064 nm beam is produced from a Coherent Mephisto 500NE with a power of up to 500 mW. The beam is coupled to a single-moded polarization-maintaining (SM/PM) fiber, which is connected to a fiber isolator via an FC-APC/SC-APC fiber-to-fiber connector. The pump light of CW 976 nm beam is produced from a Coherent DILAS I5F1P22-976.1-60C-HS7.7O2-2m laser diode with a power of up to 65 W and directly launched into a multimoded fiber (MMF). Based on simulations and observations described later, a pump power of 20 W is sufficient for the planned use. The two beams are individually coupled into the core and inner cladding of the passive double-cladded fiber (PF), respectively, at the combiner. The PF is directly spliced to an ytterbium-doped active fiber (YDF), which is then directly connected to a pigtail fiber collimator. The fiber tip and collimator are anti-reflection coated with a nominal return loss of 60 dB, and the nominal output beam is $1/e^2$-diameter 2.5 mm, with a full divergence angle of 0.6 mrad. The total length L_{fiber} of the YDF determines the gain of the YDFA, and is optimized by numerical simulation as described later.

2.3 Fabrication

Optical components such as the isolators, waveplates, the combiner, and fiber collimators are either commercially available or customly produced through Kokyo Inc. The optical fibers were fusion-spliced with each other using a Fujikura FSM-100+ fusion splicer. The splice points were covered with protection sleeves to prevent accidental breaking, except for the splice points of the PF and YDF, since the high refractive index causes the light to leak. The splice points are instead recoated using a Fujikura FSR-05 recoater wherever possible, and otherwise simply fixed onto a metal plate without any covering. The detailed configurations are tabulated in Table 1.

Table 1 Fiber properties of the upstream and downstream side, and coating treatment of each splice point. Abbreviations are *SM/PM*: Corning PM98 (Core MFD 6.6(5) μm, NA unspecified), *MMF1*: Nufern FUD-4309, Revision: B (Core 106.5 μm, NA0.2–0.24), *MMF2*: Nufern 105 Micron Core Power Delivery Fibers (Core 105(3) μm, NA0.22(2)), *PF*: Nufern Precision Matched Passive Polarization Maintaining Large Mode Area Double Clad Fibers (core 11(1) μm, NA0.075(5), inner cladding 125(1) μm, NA≥0.46), *YDF*: Nufern Precision Matched Active Polarization Maintaining Large Mode Area Double Clad Fibers (core 11(1) μm, NA0.075(5), inner cladding 125(1) μm, NA≥0.46), and *HPC*: OZ Optics PC-04-1060-10/125-P-3.4-18AS-60-X-1-1-HPC collimator

Splice point	Upstream fiber	Downstream fiber	Coating
1	SM/PM with SC/APC fiber connector	SM/PM	Protection sleeve
2	SM/PM	SM/PM	Protection sleeve
3	MMF1	MMF2	Protection sleeve
4	PF	YDF	Reacoating
5	YDF	YDF with HPC	Bare

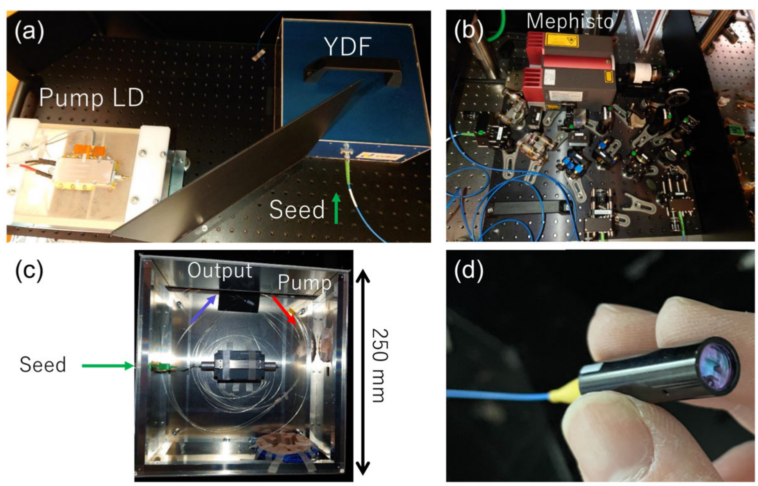

Figure 2 Components of the fabricated YDFA, comprised of (a) the pump LD on a peltier stage and the YDF contained in an aluminum box, and (b) the seed laser generated with a Mephisto LD and coupled into an optical fiber. (c) shows the inside of the box containing a fiber-based isolator and a combiner (located at the center of the box) along with the YDF itself. (d) shows the collimator attached at the end of the YDF

The components from the in-line isolator to the second splice point of the YDF are contained in a custom-made aluminum box, so that they are protected from accidental breaking or dust. The actual image of each component can be seen in Fig. 2.

3 Numerical modeling

3.1 Formulation

The population rate equations and power propagation equations are based on the formulation of Equations 1-5 of Ref. [11]. The Yb^{3+} dope rate per volume n_{Yb} is a parameter unique to each Yb-doped fiber and was found to greatly affect the result. Based on the information by the manufacturer, the value was altered to $n_{\mathrm{Yb}} = 1.1 \times 10^{26}\ \mathrm{m}^{-3}$.

As an additional consideration, three dimensionless parameters ε_S, ε_P, and ε_r, were introduced to account for the effective coupling efficiencies of the seed and pump beams into the YDF, and the rate of the amplified light being reflected at the output end of the YDFA, respectively. Since the pump laser source is spliced to the YDF, ε_P should be close to unity, but we found that it is around 80%. We suspect the origins of this to be the slight

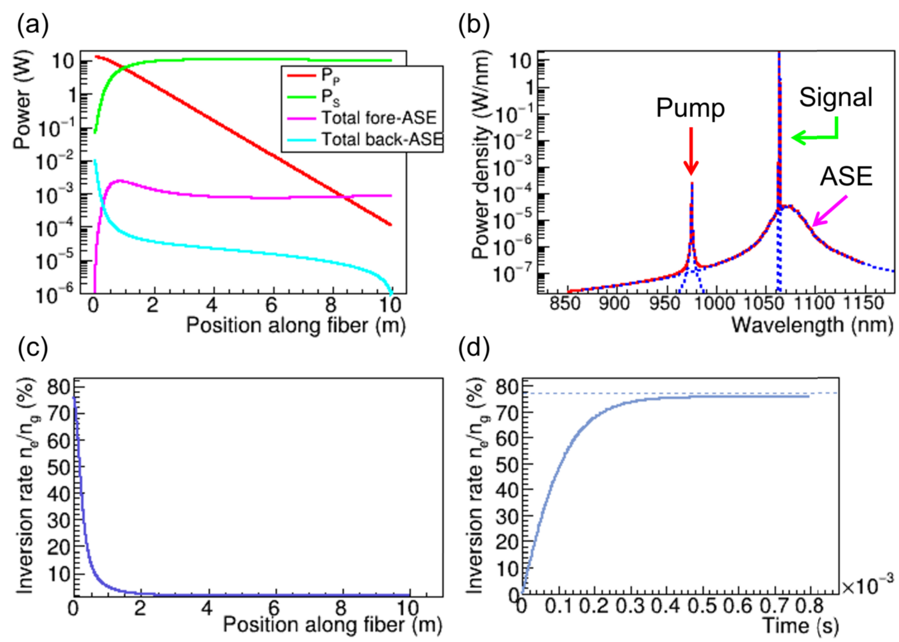

Figure 3 Result of a numerical simulation with the parameters shown in Table 2. (a) Power of each beam (pump: P_P, signal: P_S, forward and backward ASE's) at each position along the YDF. The pump and signal beams are injected at position 0 (with powers 13 W and 0.2 W, respectively), and the signal is enhanced as the pump is absorbed. The power at the end of the fiber (position 10 m) is what is ejected. (b) Optical spectrum of the output beam, consisting of the depleted pump, enhanced signal, and the (forward) ASE. (c) Population inversion rate at each position along the YDF. (d) Time dependence of population inversion rate at fiber input. Broken line represents the steady-state solution with ASE disregarded

differences in core diameter and numerical apertures, as well as the quality of the fusion splicing and recoating. When ε_r is not zero, part of the amplified seed light is backwardly propagated through the fiber and is emitted at the input end.

3.2 Design optimization

Figures 3 show calculation results for the parameter set tabulated in Table 2. The above formulation is integrated by the Euler method, using a code programmed in C++ language with the help of the ROOT library [12]. The YDF length step δL and time step δt were each set to 2 mm and 0.3 ms for a typical calculation, and was carefully re-tuned whenever the calculation diverged. Figure 3(a) shows the resulting power at each position of the fiber. As the seed and pump beams propagate from the input end of the YDF, the pump is absorbed and the seed is enhanced. At approximately 5 m, the pump is almost completely absorbed and the enhancement of the seed saturates. Beyond that, the seed light propagates only with a slight decay through linear loss. The forward and backward amplified spontaneous emission (ASE) components are also calculated, but they do not contribute significantly in terms of power in our choice of wavelengths, as observed in Ref [1]. Practically, SBS will become non-negligible when the YDF is too long [6]. Accordingly, the length of the YDF L_{fiber} is adjusted to be 4.7 m, so that the amplification gain is maximized, while the risk for SBS is minimized. By launching a pump light of approximately 13 W optical power, the signal will be amplified to more than 10 W.

Figure 3(b) shows the resulting optical spectrum, by approximating each wavelength component with a Lorentzian distribution. By taking into account the absorption and

Table 2 Parameters used for the simulation in Fig. 3

Parameter	Value
Yb^{3+} ion density $n_{Yb} = n_e + n_g$	1.1×10^{26} /m^3
Loss rate α_{loss}	6.3×10^{-3} /m
Excited state lifetime $\tau_{Yb^{3+}}$	0.8 ms
Effective fiber core area A_{fiber}	1.2×10^{-10} m^2
Time step δt	0.8 μs
Time limit t_{limit}	0.8 ms
Length step δL	2 mm
Fiber length L_{fiber}	10 m
ASE bandwidth per channel $\Delta\lambda_{ASE}$	6.6 nm
ASE wavelength range	864–1194 nm
ASE channels	51
Pump spectrum channels	5
Seed power P_S	0.2 W
Pump power P_P	13 W
Seed input efficiency ε_S	30%
Pump input efficiency ε_P	80%
Return loss ε_r	0%

emission spectrum of the YDF, the ASE can be estimated to appear on the longer-wavelength side of the 1064 nm signal. In this particular calculation, the signal gain is 22 dB, whereas the signal-to-noise ratio is 57 dB. The noise figure is calculated to be 5.9 dB, assuming that the seed beam does not contain any noise.

When the length step δL or time step δt is inadequately large, either the final values of the population inversion rate at each segment (Fig. 3(c)) or the temporal trend of the population inversion rate at the input end of the YDF (Fig. 3(d)) shows an unphysical oscillation or divergence. In such occasion, we decrease the steps until they are cured. In the current situation where the ASE level is small, the population inversion rate is expected to saturate near the broken line, which is the steady-state solution calculated without including ASE effects.

4 Experiment

4.1 Power characteristics

The power of the output beam from the YDFA was measured for various pump powers, using a power meter (Coherent, FieldMate). The result is shown in Fig. 4. The seed power was fixed at 0.2 W. The solid line is a numerical simulation which is not a fit to the data, but the parameters are fine-tuned in the following way. First, only the seed light was launched into the YDFA and the output power was measured as a function of the injection current of the seed laser source. This was compared to the numerical simulation with $\varepsilon_S = 1$ and $\varepsilon_P = 0$, which could be approximately modeled with an order-six polynomial. The polynomial was then fitted to the experimental data with an additional factor ε_S, to determine the overall coupling efficiency of the seed light. Next, the seed and pump powers were scanned by adjusting the injection currents in discrete steps. The parameter ε_P is fine-tuned by hand by comparing the numerical simulation and the experimental data when the seed and pump beams are both launched into the YDF at powers approximately 0.07 W and 4 W, respectively. Finally, the whole trend is compared between experiment and calculation, and the parameter ε_r is fine-tuned to account for the slight non-linearity in the high-power end.

The result shows that the YDFA is capable of producing over 10 W of power, consistent with the expected outcome from the simulation in Fig. 3. The trend also reasonably

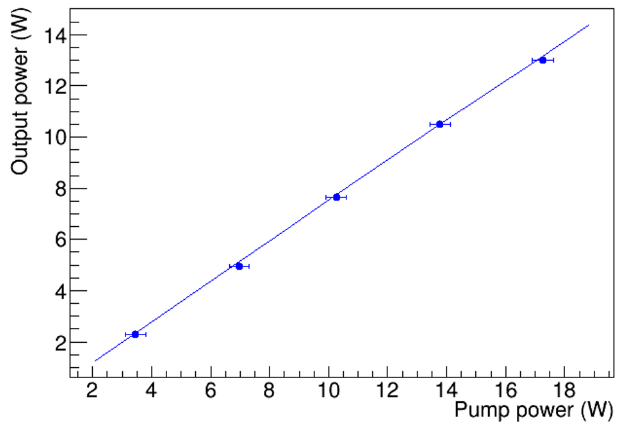

Figure 4 Pump power characteristics of the developed YDFA. Curve represents the numerical simulation with the parameters $L_{\mathrm{fiber}} = 4.7\ \mathrm{m}$, $(\varepsilon_S, \varepsilon_P, \varepsilon_r) = (0.326, 0.8, 0.02)$, and $P_S = 0.2\ \mathrm{W}$. Horizontal axis is the optical power launched into the YDF, *i.e.* $\varepsilon_P P_P$

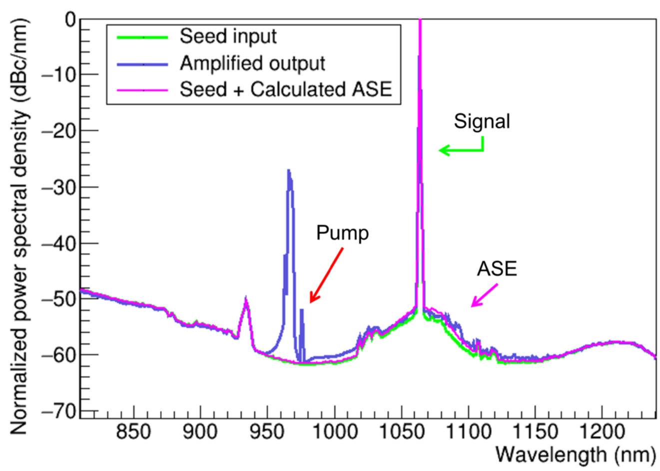

Figure 5 Normalized optical spectrum of the YDFA output for seed optical power $P_S = 0.2\ \mathrm{W}$ and pump optical power $P_P = 5\ \mathrm{W}$. The YDF length is $L_{\mathrm{fiber}} = 4.7\ \mathrm{m}$

matches with numerical simulation, which indicates that the naive model is an adequate representation of the YDFA, and there is no significant contribution of SBS at this power level.

4.2 Spectral characteristics

The optical spectrum of the output light is observed by picking off approximately 3% of the beam using a glass plate and coupling it to a SM/PM fiber connected to the optical spectrum analyzer (OSA; Anritsu MS9740A). The remaining power is dumped into a beam block.

Figure 5 shows the resulting normalized optical spectra of the seed light itself and the output of the YDFA. Since the output signal is expected to be a sum of the seed spectrum and the ASE, the calculated ASE spectrum added to the seed spectrum is also drawn as the "calculated" spectrum.

As already predicted by the numerical simulation, the ASE has a negligibly small contribution to the output beam. Meanwhile, there is a large peak at around 970 nm, which differs from the 976 nm pump wavelength. This has been confirmed to originate from the pump laser source itself, and does not seem to contribute largely to the amplification nor the gain loss of the 1064 nm seed beam.

4.3 Mode characteristics

The spatial mode of the beam emitted from the YDFA plays an important role in determining the geometry of the optical trap, as well as the transmission rate of the beam to the experimental setup through SM/PM fibers. The mode has not been explicitly measured due to the high power, but it has been confirmed that approximately 50 % of the beam can be coupled to a SM/PM fiber when the beam is transmitted through an optical isolator.

5 Conclusion

We have developed a YDFA capable of producing a CW laser of 1064 nm over 10 W of power. This power is sufficient to form an optical lattice trap of the depth equivalent to more than 0.2 mK. As it is self-constructed using the fiber splicing technique, rapid maintenance and flexible customization have become possible. This serves as an example of a high-power laser source that is to be used in harsh environments such as a radiation controlled areas. Meanwhile, studies on possible improvements of radiation hardness for optoelectric devices used in high-energy colliders are also conducted [4]. By using our strategy, the installed components can be easily replaced with devices having less vulnerability to radiation. As laser cooling and trapping techniques serve as one of the powerful tools for precision measurements, including the electron EDM search utilizing Fr atoms, our work is expected to benefit such schemes.

Acknowledgements
The authors wish to acknowledge Prof. H. Katori and Dr. A. Yamaguchi along with the members of the Quantum Metrology Laboratory of RIKEN, Dr. Y. Imai of Okayama University, Fujikura Inc., and Kokyo Inc. for technical support.

Author contributions
NO: Conceptualization, Investigation, Analysis, Validation, Writing—Original Draft. KN: Conceptualization, Investigation, Analysis, Validation, Writing—Review and Editing. YS: Writing—Review and Editing, Supervision. All authors read and approved the final manuscript.

Funding
The authors are grateful for the financial supports from JSPS KAKENHI Grant Nos. 19H05601, 20K14482, 21J12044, and 22K18273, as well as the Murata Science Foundation, and the JSR Fellowship of the University of Tokyo.

Data availability
The data that supports the findings of this study are available from the corresponding author upon reasonable request.

Declarations

Competing interests
The authors declare that they have no competing interests.

Author details
[1]Graduate School of Science, University of Tokyo, Hongo 7-3-1, Bunkyo, 113-0033, Tokyo, Japan. [2]Center for Nuclear Study, University of Tokyo, Hirosawa 2-1, Wako, 351-0198, Saitama, Japan. [3]*Present address:* Graduate School of Science, Kyoto University, Kita-Shirakawa-Oiwake-cho, Sakyo, 606-8502, Kyoto, Japan.

Received: 13 September 2023 Accepted: 29 March 2024 Published online: 04 April 2024

References

1. Paschotta R, Nilsson J, Tropper AC, Hanna DC. Ytterbium-doped fiber amplifiers. IEEE J Quantum Electron. 1997;33:1049.
2. Jeong Y, Nilsson J, Sahu JK, Payne DN, Horley R, Hickey LMB, Turner PW. Power scaling of single-frequency ytterbium-doped fiber master-oscillator power-amplifier sources up to 500 W. IEEE J Sel Top Quantum Electron. 2007;13(3):546–51. https://doi.org/10.1109/jstqe.2007.896639.
3. Zhang L, Cui S, Liu C, Zhou J, Feng Y. 170 W, single-frequency, single-mode, linearly-polarized, Yb-doped all-fiber amplifier. Opt Express. 2013;21(5):5456. https://doi.org/10.1364/oe.21.005456.
4. Hou S, Ishii K, Itoh M, Sakemi Y, Su DS, Su TT, Teng PK, Yoshida HP. Radiation hardness of optoelectronic components for the optical readout of the ATLAS inner detector. Nucl Instrum Methods Phys Res, Sect A, Accel Spectrom Detect Assoc Equip. 2011;636(1):137–42.
5. Nakamura N, Nagase S, Nakashita T, Hayamizu T, Aoki T, Nagahama H, Ozawa N, Sato M, Yamane K, Fukase M, Uehara D, Takamine A, Sakemi Y. 400-m-long polarization-maintaining fibers for magneto-optical trapping of francium atoms. In: Proceedings of the 2022 conference on lasers and electro-optics Pacific rim 7–03. 2022
6. Agrawal GP. Nonlinear fiber optics. 2nd ed. San Diego: Academic Press; 1995.
7. Sakemi Y, Harada K-I, Itoh M, Ito S, Uchiyama A, Inoue T, Kawamura H, Aoki T, Hatakeyama A, Takahashi Y, Hisano J. Fundamental physics with cooled radioactive atoms. In: Proceedings of 10th international conference on nuclear physics at storage rings (STORI'17). vol. 35. 2021. p. 011016.
8. Ozawa N, Nagahama H, Sakemi Y. Francium ion source with novel methods of target heating and beam characterization. Rev Sci Instrum. 2023;94:023306.
9. Ozawa N. Development of a surface ionizer for the francium electric dipole moment search. Master's thesis. University of Tokyo; 2020. (in Japanese).
10. Singleton BJ. Radiation effects on ytterbium-doped optical fibers. PhD thesis. Air Force Institute of Technology; 2014. https://scholar.afit.edu/etd/530.
11. Budz AJ, Waisman J, Tiedje HF, Haugen HK. Short-pulse dual-wavelength system based on mode-locked diode lasers with a single polarization-maintaining Yb:fiber amplifier. J Lightwave Technol. 2009;27:3416.
12. Brun R, Rademakers F. ROOT—an object oriented data analysis framework. Nucl Instrum Methods Phys Res, Sect A, Accel Spectrom Detect Assoc Equip. 1997;389(1–2):81–6. https://doi.org/10.1016/s0168-9002(97)00048-x.

Publisher's Note